Effect of the α-nucleus interaction on the ^{29,30}Si$(\alpha,d)^{31,32}$P reaction

S. K. Das,[1] A. S. B. Tariq,[1] A. F. M. M. Rahman,[1] S. Hossain,[1] A. S. Mondal,[1] A. K. Basak,[1] H. M. Sen Gupta,[2] and F. B. Malik[3]

[1]*Department of Physics, University of Rajshahi, Rajshahi, Bangladesh*

[2]*Department of Physics, University of Dhaka, Dhaka, Bangladesh*

[3]*Department of Physics, Southern Illinois University, Carbondale, Illinois 62901*

(Received 3 March 2001; published 16 August 2001)

Microscopic and macroscopic distorted wave Born approximation calculations have been performed using the molecular, standard Woods-Saxon (WS), and squared WS (Michel) α-nucleus potentials to analyze the angular distributions of cross sections for nine transitions to the even-parity states up to excitation energy $E_x=4.26$ MeV of ^{31}P and eight transitions to the even-parity states up to $E_x=3.00$ MeV of ^{32}P populated in the (α,d) reaction at 25 MeV incident energy on the non-α cluster ^{29,30}Si nuclei. The parameters of the three types of the α-nucleus potentials are determined from the elastic α-scattering data. The molecular potential, without any adjustment to the parameters needed to fit the elastic scattering data, is able to reproduce, simultaneously, the absolute cross sections and the pattern of angular distributions, but the WS and Michel potentials, obtained from the best fits to the elastic scattering data, are found to underestimate the cross sections by one to two orders of magnitude. The spectroscopic factors for the *d*-cluster transfer are deduced from the full finite-range macroscopic distorted-wave Born approximation, for nine and eight transitions to states in ^{31}P and ^{32}P, respectively, using all three potentials and are compared to those calculated by the shell model, which agree with those deduced from the fits to the data using the molecular potential only.

DOI: 10.1103/PhysRevC.64.034605 PACS number(s): 24.50.+g, 21.10.Jx

I. INTRODUCTION

The anomalous large angle scattering (ALAS) observed in the elastic scattering of α particles [1–9] as well as in the nonelastic processes involving α particles [7–15] cannot be explained by the standard optical potential with Woods-Saxon (WS) geometry [5,16]. ALAS in the elastic scattering, however, can be accounted for by two simple types of the α-nucleus local potential. The first one, a squared WS potential due to Michel and co-workers [17–20], is usually referred [21,22] to as the Michel potential and the second is a nonmonotonic molecular potential [21,23,24] with a short-range repulsive core. Both the potentials have been successful in accounting for ALAS in the inelastic scattering of α particles by ^{24}Mg and ^{28}Si [25] and the one-nucleon transfer (α,t) reaction on ^{27}Al [22]. However, only the molecular potential, with the same parameters as those obtained from fitting the elastic scattering data, provides a proper description of the two-nucleon transfer (α,d) process [26] and the three-nucleon transfer (α,p) [27] reaction on ^{28}Si.

The present work is a continuation of our investigations on the effect of α-nucleus potentials on various reaction processes and targets. So far, our analyses on the two- and three-nucleon transfer reactions have been restricted to ^{28}Si, which is an ''α-cluster nucleus,'' meaning that its constituents can be construed as multiple α particles. In this paper, we extend our investigation to the ''non-α cluster nuclei,'' ^{29,30}Si using the usual WS, Michel, and molecular potentials within the framework of microscopic and macroscopic distorted wave Born approximation (DWBA). Davis and Nelson failed to explain their (α,d) data at 25 MeV incident energy on ^{29,30}Si [28] using the same optical model parameters as those needed to explain the elastic scattering data and had to vary them significantly to forge fits to the (α,d) reaction data. The present work examines how well the unadjusted parameters of the molecular, standard WS, and Michel potentials in the α channel, obtained from fitting the elastic scattering data, can account for the data of the ^{29,30}Si$(\alpha,d)^{31,32}$P reactions. In Sec. II, the forms of the three α-nucleus potentials used in the present work are presented. The DWBA formalism and analyses are discussed in Secs. III and IV, respectively. Section V deals with the discussion on the result of the analyses. The conclusion is given in Sec. VI.

II. α-NUCLEUS POTENTIALS

The complex squared WS Michel potential [18,19] including the Coulomb term $V_C(r)$ comprises the following forms [18,21] of the real $V_M(r)$ and imaginary $W_M(r)$ parts:

$$V_M(r)=-V_0\left\{1+\alpha\exp\left[-\left(\frac{r}{\rho}\right)^2\right]\right\}\left[1+\exp\left(\frac{r-R_R}{2a_R}\right)\right]^{-2}+V_c(r), \tag{1}$$

$$W_M(r)=-W_0\left[1+\exp\left(\frac{r-R_W}{2a_W}\right)\right]^{-2}, \tag{2}$$

with

$$V_C(r)=\left[\frac{Z_1Z_2e^2}{2R_C}\right]\left[3-\frac{r^2}{R_C^2}\right] \quad \text{for} \quad r\leqslant R_C \tag{3}$$

$$=\frac{Z_1Z_2e^2}{r} \quad \text{for} \quad r>R_C. \tag{4}$$

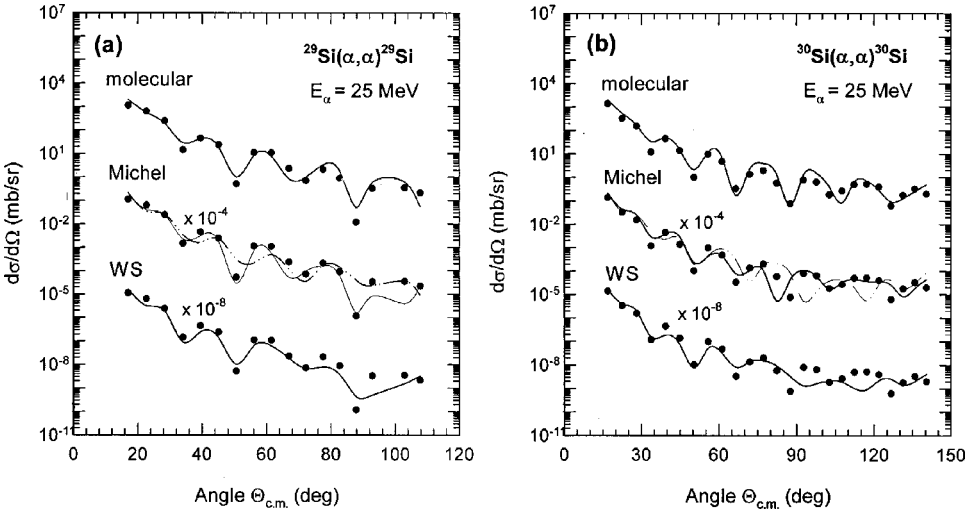

FIG. 1. Fits to the α elastic scattering data at 25 MeV (laboratory) for (a) ^{29}Si and (b) ^{30}Si with the molecular, Michel, and standard WS potentials. Solid curves are the predictions for elastic best-fit parameters. The broken curves are for the adjusted α and W_0 Michel parameters for the reduced real volume integral. Data are from Refs. [28,29].

In Eqs. (1)–(4), $R_i = r_i A_T^{1/3}$ (A_T is the mass number of the target and $i = R, W, C$), a_i ($i = R, W$), and ρ are the geometry parameters. V_0, W_0, and α represent the strengths of the potential. Z_1 and Z_2 are the charges of the projectile and target, respectively.

The molecular potential has the following forms [21,22,24] for the real $V_m(r)$ and imaginary $W_m(r)$ parts:

$$V_m(r) = -V_0\left[1+\exp\left(\frac{r-R_R}{a_R}\right)\right]^{-1} + V_1\exp\left[-\left(\frac{r}{R_1}\right)^2\right] + V_C(r), \tag{5}$$

$$W_m(r) = -W_0\exp\left[-\left(\frac{r}{R_W}\right)^2\right]. \tag{6}$$

Thus, the real part is nonmonotonic with a short-range repulsive potential of range R_1 and depth V_1.

The standard WS potential for the α-nucleus system including the Coulomb term is given by

$$V(r) = V_C - Vf(x_R) - i\left[Wf(x_W) - 4W_D\frac{d}{dx}f(x_D)\right]. \tag{7}$$

Here, $f(x_i) = (1+e^{x_i})^{-1}$, where $x_i = (r-R_i)/a_i$ with $R_i = r_i A_T^{1/3}$ ($i = R, W, D$).

The parameters for the molecular, standard WS, and Michel types of the α-^{29,30}Si potential at the 25 MeV incident energy are obtained from the best fit to the elastic scattering data [29] using the χ^2 minimization code MINUIT [30] coupled with the optical model code SCAT2 [31] modified to incorporate the molecular and Michel potentials. The initial parameters for the WS potential are taken from Davis and Nelson [28]. For the molecular and Michel potentials, the parameters of the α-^{28}Si potential from Tariq *et al.* [21] are considered as the starting parameters for the α-^{29,30}Si interaction. The fits to the elastic data are shown in Fig. 1. The parameters of the molecular, Michel, and WS potentials are noted in Table I.

III. THEORY OF DWBA FORMALISM

In the absence of spin-orbit interactions, the differential cross section for an (α,d) reaction in the DWBA theory with a full finite-range interaction is given by [32]

$$\frac{d\sigma}{d\Omega} = \frac{\mu_i\mu_f}{(2\pi\hbar^2)^2}\frac{k_f}{k_i}\frac{(2J_f+1)}{(2J_i+1)} \times \sum_{JLM}\left|\sum_{\rho_1\rho_2}\beta^{1/2}[\rho_1\rho_2;J0]\begin{bmatrix} l_1 & l_2 & L \\ \frac{1}{2} & \frac{1}{2} & 1 \\ j_1 & j_2 & J\end{bmatrix}B_M^L\right|^2. \tag{8}$$

In Eq. (8) μ's and k's are, respectively, the reduced masses and wave numbers. The subscripts i and f refer to the incident and outgoing channels, respectively. J is the total angular momentum transfer. $\rho_1 = [n_1 l_1 j_1]$ and $\rho_2 = [n_2 l_2 j_2]$ denote the orbital quantum numbers for the transferred nucleons in the final nucleus. $\beta^{1/2}[\rho_1\rho_2;J0]$ are the spectroscopic amplitudes in the jj coupling for an angular momentum transfer J and an isospin transfer $T=0$. The large square bracket refers to the normalized 9-j symbol involving the transformation from the LS to jj coupling scheme [33]. B_M^L describes the kinematical aspects of the reaction. In Eq. (8) the light-particle spectroscopic factor c^2s is set to be 1.0.

In the macroscopic DWBA calculations, no information on the structure of the cluster is required except the quantum numbers (N,L), which are defined by

$$2(n_1+n_2)+l_1+l_2 = 2N+L. \tag{9}$$

In Eq. (9), the relative $0s$-state internal motion of the transferred cluster is assumed. This means that a particular L value corresponds to only one value of N. The expression for cross section in terms of the cluster quantum numbers (N,L) parallel to Eq. (8) is given by [33]

TABLE I. Potential parameters for DWBA calculations. The potential depth V for the bound states is adjusted to give the separation energy of bound deuteron in α and final nucleus.

Channel	$\alpha+^{29}$Si			$\alpha+^{30}$Si			$d+^{31,32}$P	$d+d$	$d+^{29,30}$Si
Potential type	Molecular	Michel	WS	Molecular	Michel	WS	WS	Bound state	
V_0 (MeV)	26.3	31.4	182.5	27.0	25.0	190.8	102.7	V	V
R_R (fm)	5.45	4.83	3.53	5.52	5.20	3.57	-	-	-
r_R (fm)	-	-	-	-	-	-	1.07	1.05	0.935
a_R (fm)	0.34	0.55	0.76	0.34	0.46	0.73	0.852	0.50	0.997
V_1 (MeV)	42.5	-	-	42.0	-	-	-	-	-
R_1 (fm)	2.90	-	-	2.90	-	-	-	-	-
α	-	7.39	-	-	7.12	-	-	-	-
ρ (fm)	-	6.45	-	-	6.45	-	-	-	-
W_0 (MeV)	17.9	34.9	13.5	17.0	34.0	13.0	17.0	-	-
R_W (fm)	4.10	4.06	4.64	4.10	4.05	4.69	4.10	-	-
a_W (fm)	-	0.64	0.70	-	0.65	0.87	-	0.65	0.87
W_D (MeV)	-	-	-	-	-	-	16.10	-	-
r_D (fm)	-	-	-	-	-	-	1.53	-	-
a_D (fm)	-	-	-	-	-	-	0.574	-	-
V_{SO} (MeV)	-	-	-	-	-	-	6.00	-	-
r_{SO} (fm)	-	-	-	-	-	-	1.07	-	-
a_{SO} (fm)	-	-	-	-	-	-	0.852	-	-
r_C (fm)	-	-	-	-	-	-	1.15	1.25	1.30
R_C (fm)	9.45	3.99	3.99	9.46	4.04	3.73	-	-	-

$$\frac{d\sigma}{d\Omega}=\frac{\mu_i\mu_f}{(2\pi\hbar^2)^2}\frac{k_f}{k_i}\frac{(2J_f+1)}{(2J_i+1)}\sum_{JLM}|G_{LJ}\Re_M^L|^2. \tag{10}$$

In Eq. (10), the structure amplitude G_{LJ}, as defined by Glendenning [33] is expressed as

$$G_{LJ}=\sum_{\rho_1\rho_2}(2-\delta_{\rho_1\rho_2})^{1/2}\beta^{1/2}[\rho_1\rho_2;J0]\times\begin{bmatrix} l_1 & l_2 & L \\ \frac{1}{2} & \frac{1}{2} & 1 \\ j_1 & j_2 & J \end{bmatrix}\Omega_{00}\langle 00,NL:L|n_1l_1,n_2l_2:L\rangle. \tag{11}$$

In Eq. (11), Ω_{00} denotes the overlap of the spatial wave function of relative motion of the two particles in the transferred cluster with the corresponding part in the incident α particle. $\langle\ |\ \rangle$ represents the Brody-Moshinsky bracket [32–34].

The reduced cross section can be defined by

$$\left(\frac{d\sigma}{d\Omega}\right)^L=\frac{\mu_i\mu_f}{(2\pi\hbar^2)^2}\frac{k_f}{k_i}\sum_M|\Re_M^L|^2, \tag{12}$$

which is proportional to $(d\sigma/d\Omega)^L_{\mathrm{DW5}}$, the cross section calculated by the code DWUCK5 [35]. In terms of the reduced cross section, Eq. (8) can be recast in the form

$$\frac{d\sigma}{d\Omega}=\frac{(2J_f+1)}{(2J_i+1)}\sum_{LJ}|G_{LJ}|^2\left(\frac{d\sigma}{d\Omega}\right)^L. \tag{13}$$

The square of the structure factor $|G_{LJ}|^2$ denotes the strength of the reactions and is proportional to the spectroscopic factor [36] of the two-nucleon (α,d) reaction.

In the macroscopic model calculations, the differential cross section for the direct transfer with multiple J transfers can be written with the incoherent sum over L transfers as

$$\frac{d\sigma}{d\Omega}=\frac{(2J_f+1)}{(2J_i+1)}\sum_{LJ}S_{LJ}\left(\frac{d\sigma}{d\Omega}\right)^L_{\mathrm{DW5}}. \tag{14}$$

Here, S_{LJ} denotes the macroscopic spectroscopic factor for the transfer (L,J). The dependence of the reduced cross section over J is dropped in the assumed absence of spin-orbit interaction resulting in the incoherent sum over L.

The spectroscopic factor for the d-cluster transfer is considered unity for a transfer to a stretched configuration ($L=l_1+l_2, J=j_1+j_2, J=L+S$), when the spectroscopic amplitude $\beta^{1/2}=1.0$, where none of the target nucleons occupies either the (l_1,j_1) or (l_2,j_2) orbital. Denoting the strength factor in Eq. (13) for such a reference state with the stretched configuration by $|G^{\mathrm{str}}_{\mathrm{ref}}|^2$, one can define the shell-model spectroscopic factor [36] for the cluster transfer as

$$S^G_{LJ}=\frac{|G_{LJ}|^2}{|G^{\mathrm{str}}_{\mathrm{ref}}|^2}. \tag{15}$$

Using a state of the final nucleus populated by the $J^\pi = 7^+ (L=6, J=7)$ transfer with the $(0f_{7/2})^2$ configuration as a reference state [36], one can calculate the theoretical spectroscopic factor from the expression

$$S_{LJ}^G = \frac{|G_{LJ}|^2}{|G_{67}^{\rm str}|^2}. \tag{16}$$

In the (α,d) reaction, the spin transfer $S=1$ is unique. Since Eq. (9) assumes that the relative angular momentum of the two transferred nucleons is 0 and remains so during the interaction responsible for the transfer, two L-transfer values given by $L_1 = J-1$ and $L_2 = J+1$ are permitted for transition to excited states with unnatural parity transfers, but only the L-transfer value $L=J$ occurs for transition with a natural parity transfer. The ground state spins of ^{29}Si and ^{30}Si being $J_i = \frac{1}{2}$ and 0, the number of allowed J transfers are, respectively, 2 and 1. In the former case, one of the J transfers with unnatural parity involves two L values, L_1 and L_2, and in case of the J transfer with natural parity, only one L, equal to one of L_1 and L_2, contributes. Thus for both ^{29,30}Si targets, there will be at best two distinct L transfers. If one denotes the cross sections predicted for the two L values in the macroscopic calculations by the full finite-range (FFR) code DWUCK5 [35], respectively, by $(d\sigma/d\Omega)_{\rm DW5}^{L_1}$ and $(d\sigma/d\Omega)_{\rm DW5}^{L_2}$ and taking advantage of the incoherent sum over the L transfers as in Eq. (14), one can write the experimental cross section as

$$\left(\frac{d\sigma}{d\Omega}\right)_{\rm expt} = \frac{(2J_f+1)}{(2J_i+1)}\left[A_{L_1}\left(\frac{d\sigma}{d\Omega}\right)_{\rm DW5}^{L_1} + A_{L_2}\left(\frac{d\sigma}{d\Omega}\right)_{\rm DW5}^{L_2}\right]. \tag{17}$$

Thus, one can deduce the spectroscopic factors A_{L_1} and A_{L_2} for the (α,d) reaction by comparing the predicted cross sections with the experimental data. The experimentally deduced total spectroscopic factor is then

$$A = A_{L_1} + A_{L_2}. \tag{18}$$

On the other hand, the theoretical spectroscopic factor S_L^G for the L transfer and its total S^G for a transition may be calculated, respectively, from the expressions

$$S_L^G = \sum_J S_{LJ}^G \tag{19}$$

and

$$S^G = \sum_L S_L^G. \tag{20}$$

Denoting the cross sections for a J transfer calculated with the zero-range (ZR) code DWUCK4 [35] by $(d\sigma/d\Omega)_{\rm DW4}^J$, one can write the experimental cross section as

$$\left(\frac{d\sigma}{d\Omega}\right)_{\rm expt} = \aleph \frac{(2J_f+1)}{(2J_i+1)} \sum_J \frac{1}{2J+1}\left(\frac{d\sigma}{d\Omega}\right)_{\rm DW4}^J. \tag{21}$$

$\aleph$ in Eq. (21) is the normalization constant for the (α,d) reactions. In the microscopic calculations, $(d\sigma/d\Omega)_{\rm DW4}^J$ in Eq. (21) involves the shell-model spectroscopic amplitudes $\beta^{1/2}$. Thus, the microscopic predictions, when compared to the experimental cross sections, can provide a test of a shell-model calculation through the coherent effects of different terms in the wave functions of the initial and final nuclei. The macroscopic approach, on the other hand, does not associate the calculated $(d\sigma/d\Omega)_{\rm DW5}^L$ in Eq. (17) with the spectroscopic amplitudes, but offers a method to deduce the spectroscopic factors A_L (in the approximation of neglecting spin-orbit interaction) from the experimental cross-section data. These extracted spectroscopic factors may then be compared to those calculated from the shell-model $\beta^{1/2}$ values using Eqs. (11) and (16).

IV. DWBA ANALYSIS

The microscopic ZR and macroscopic FFR DWBA calculations for the angular distributions have been performed using the computer codes DWUCK4 and DWUCK5 [35], respectively. Both the codes are modified to include the Michel potential. Corrections due to nonlocality [35,38] of potentials in the conventional form have been applied using the nonlocality parameters $\beta(\alpha)=0.2$, $\beta(d)=0.54$, and $\beta(p)=0.85$ fm. In both the microscopic ZR and macroscopic FFR calculations, the molecular, Michel, and standard WS potentials, obtained from the best fits to the scattering data, have been used in the α channel, and the WS potential has been employed in the d channel. The parameters of the three types of α-Si potential are displayed in Table I. Several sets of WS potentials in the d channel have been tried, but only the one from the work of Fitz *et al.* [39] produces a good fit for both the targets.

A. Macroscopic DWBA calculations

The macroscopic analyses have been performed using the full finite-range DWBA code DWUCK5 [35]. The bound-state geometries (r_R and a_R) for the d-d and d-^{29,30}Si WS potentials shown in Table I are taken from Ref. [37]. The geometrical parameters of the latter potentials are kept the same as those for the d-^{28}Si potential. The bound-state wave functions for the transferred deuteron, in the α and in the final nucleus, have been generated by adjusting the depth of the WS well for the correct deuteron separation energies. At the start of calculations, the ''accuracy parameters'' used in the code DWUCK5, which control the effective width of wave numbers [35,40] in the expansion of the distorted waves in terms of plane waves, have been assigned appropriate values for making the predictions of zero-range calculations identical to those calculated from the zero-range code DWUCK4 [35]. This ensures the necessary ''convergence'' for the integral for the zero-range form factor, defined in Eq. (3.9) of Charlton [40].

The cluster configurations of the transferred deuteron for the different states of excitation are shown in Table II. For the final states with natural parity populated by one L transfer, the DWBA predictions are normalized to the data to yield the relevant spectroscopic factor A_L as defined in Eq. (17). On the other hand, for the transitions involving two L transfers, the spectroscopic factors are obtained by minimizing the χ^2 defined by

$$\chi^2=\sum_i \left[\frac{\sigma_{\rm expt}(\theta_i)-\sigma_{\rm DW}(\theta_i)}{\Delta\sigma_{\rm expt}(\theta_i)}\right]^2, \qquad (22)$$

where $\sigma_{\rm expt}(\theta_i)=(d\sigma/d\Omega)_{\rm expt}(\theta_i)$ and $\Delta\sigma_{\rm expt}(\theta_i)$ are, respectively, the experimental cross section, as defined in Eq. (17), and its error at the scattering angle θ_i. $\sigma_{\rm DW}(\theta_i)$ is the cross section predicted by the DWBA theory.

The DWBA predictions with the molecular (solid curves), standard WS (broken curves), and Michel (dotted curves) potentials are compared to the reaction data on ^{29}Si for the ground $(1/2^+)$, 1.27 $(3/2^+)$, 2.23 $(5/2^+)$, 3.13 $(1/2^+)$, 3.30 $(5/2^+)$, 3.41 $(7/2^+)$, 3.51 $(3/2^+)$, 4.19 $(5/2^+)$, and 4.26 MeV $(3/2^+)$ states in Fig. 2(a). Similarly, for the reaction on ^{30}Si the predictions are compared to the data of the ground (1^+), 0.08 (2^+), 1.15 (1^+), 1.32 (2^+), 1.75 (3^+), 2.66 (2^+), 2.74 (1^+), and 3.00 MeV (3^+) state transitions in Fig. 2(b). The comparison of the data with calculations shown in Figs. 2(a) and 2(b) indicates that the three α-nucleus potentials provide reasonable descriptions of the data for the reaction to the various states of excitation of both ^{31,32}P, except for the 2.66 MeV (2^+) state of ^{32}P. The predictions with all three types of α-nucleus potentials can account for the observed pattern of the angular distributions of cross section up to about 90°. At larger angles, the calculated cross sections with the Michel and standard WS potentials tend to fall off faster than the data. Furthermore, the Michel and WS potentials underestimate the cross sections in many cases by one to two orders of magnitude. This is reminiscent of the ^{28}Si$(\alpha,d)^{30}$P case [26]. Unfortunately, no data beyond 120° exist in the two reactions considered herein. The calculations using the molecular potential, although failing to generate proper structure at larger angles at some instances, seem to account for the correct order of magnitude in most of the cases.

In Table II, the spectroscopic factors A_L for the cluster transfer deduced from the calculations using the three potentials, along with the values expected from shell-model calculations S_L^G, using the MSDI [44], RIP [43], and KB [41] two-nucleon matrix elements are presented. The total spectroscopic factors A, deduced from using the molecular, WS, and Michel potentials, and S^G, calculated from the two-nucleon matrix elements are compared in Table III. A values extracted from the fits to the data using the molecular potential are in reasonable agreement with the calculated S^G from the three types of matrix elements in terms of general trend and magnitude. The calculations using the MSDI matrix elements seem to agree with the deduced A values somewhat better. The A values, deduced from the use of the WS and the Michel potentials, are usually larger by one to two orders of magnitude.

B. Microscopic DWBA calculations

The microscopic calculations have been performed using the zero-range code DWUCK4 for the positive parity states with the transferred particles stripped to the sd shell. The present analyses make use of three sets [28] of shell-model spectroscopic amplitudes $\beta^{1/2}$, which are as follows.

(i) The set labeled KB uses the Kuo-Brown [41] two-body matrix elements calculated from the nucleon-nucleon interaction of Hamada and Johnston [42].

(ii) The set labeled RIP is based on the effective interaction [43] derived by fitting the observed nuclear energy levels.

(iii) The set labeled MSDI is extracted from the matrix elements of two-nucleon modified surface delta interaction [44].

Since the codes DWUCK4 and DWUCK5 assume that the spherical harmonics carry a time reversal phase of i^l, a factor not used in the phase conventions adopted in the calculations of the spectroscopic amplitudes [36], the amplitudes have been multiplied by an extra phase of $i^{l_1+l_2-L}$ before feeding these to the codes.

The bound-state wave functions for each of the transferred nucleons have been generated by assuming a real Woods-Saxon well with the geometry parameters $r_R=1.25$ fm and $a_R=0.65$ fm and the depth adjusted to produce the binding energy equal to half the separation energy of the transferred deuteron. A spin-orbit term with $\lambda=25$ has also been used for the bound-state wave functions. A finite-range correction in Gaussian form [35] with the range parameter $R=0.7$ fm is used in the microscopic DWBA calculations, since it improves the fits to the data [26].

The effects of the MSDI, RIP, and KB interactions on the predicted cross sections for the reaction on both targets are first investigated using all three potentials in the α channel. The calculated cross sections using the molecular potential only are compared to the data for the transitions on ^{29}Si and those on ^{30}Si in Figs. 3(a) and 3(b), respectively. Apart from the ground state $(1/2^+)$, 1.27 $(3/2^+)$, 3.13 $(1/2^+)$, and 3.51 MeV $(3/2^+)$ transitions [Fig. 3(a)] on ^{29}Si and the ground state (1^+), 1.15 (1^+), and 3.00 MeV (3^+) transitions [Fig. 3(b)] on ^{30}Si, the three sets of spectroscopic amplitudes calculated from the three matrix elements produce more or less similar fits. An identical situation occurs with the other two types of the α-nucleus potential, namely, the standard WS and Michel ones. However, the set of spectroscopic amplitudes, calculated using the MSDI matrix elements, seems to reproduce the data slightly better.

The effect of the three types of the α-nucleus potential on the microscopic DWBA calculations has also been examined using the spectroscopic amplitudes calculated from the MSDI interaction. Figures 4(a) and 4(b) display the predictions from the microscopic DWBA calculations for the molecular (solid curves), standard WS (broken curves), and Michel (dotted curves) potentials, and the data for the various states populated in the (α,d) reaction on ^{29,30}Si. As in the case of the macroscopic analyses, although the three α-nucleus potentials produce reasonable fits to the data for the reactions on both ^{29,30}Si, again the molecular potential

TABLE II. Cluster spectroscopic factors are compared to the theoretical shell-model factors for the MSDI, RIP, and KB interactions. The theoretical spectroscopic factors are calculated from the spectroscopic amplitudes $\beta^{1/2}$ of Refs. [28] and [29] by the method outlined in Ref. [36].

(a) Transitions in the ^{29}Si$(\alpha,d)^{31}$P reaction

E_x	J^π	Cluster configuration	Cluster spectroscopic factor A_L			Shell-model spectroscopic factor S_L^G		
(MeV)		N,L,J	Molecular	WS	Michel	MSDI	RIP	KB
0.0	$1/2^+$	2,0,1	0.18±0.06	12.6±2.6	7.2±1.4	0.611	0.027	0.024
		1,2,1	0.12±0.04	8.4±1.7	4.8±1.0	0.006	0.053	0.011
1.27	$3/2^+$	2,0,1	0.05±0.01	3.0±0.6	1.8±0.4	0.007	0.009	0.006
		1,2,1+1,2,2	0.30±0.09	4.5±0.9	2.7±0.5	0.597	0.176	0.060
2.23	$5/2^+$	1,2,2+1,2,3	0.14±0.04	5.0±1.1	1.58±0.32	0.112	0.220	0.013
		0,4,3	0.008±0.002	0.26±0.07	0.08±0.02	0.000	0.004	0.003
3.13	$1/2^+$	2,0,1	0.05±0.02	0.90±0.27	0.76±0.15	0.021	0.009	0.171
		1,2,1	0.08±0.02	1.50±0.30	1.54±0.23	0.229	0.036	0.026
3.30	$5/2^+$	1,2,2+1,2,3	0.08±0.03	4.08±0.81	3.8±0.80	0.084	0.006	0.002
		0,4,3	0.005±0.001	0.22±0.05	0.2±0.05	0.000	0.011	0.067
3.41	$7/2^+$	1,2,3	0.26±0.08	13.0±3.9	5.2±1.3	0.005	0.031	0.002
		0,4,3+0,4,4	0.03±0.01	3.25±0.65	1.3±0.33	0.143	0.020	0.101
3.51	$3/2^+$	2,0,1	0.06±0.02	1.8±0.4	1.5±0.4	0.001	0.060	0.002
		1,2,1+1,2,2	0.14±0.04	4.2±0.8	3.5±0.9	0.169	0.012	0.200
4.19	$5/2^+$	1,2,2+1,2,3	0.09±0.03	4.0±0.8	4.4±1.1	0.058	0.077	0.010
		0,4,3	0.022±0.006	1.00±0.25	1.10±0.26	0.014	0.029	0.061
4.26	$3/2^+$	2,0,1	0.07±0.02	2.8±0.7	2.20±0.55	0.002	0.004	0.002
		1,2,1+1,2,2	0.14±0.04	4.2±1.1	3.30±0.83	0.005	0.052	0.011

(b) Transitions in the ^{30}Si$(\alpha,d)^{32}$P reaction

E_x	J^π	Cluster configuration	Cluster spectroscopic factor A_L			Shell-model spectroscopic factor S_L^G		
(MeV)		N,L,J	Molecular	WS	Michel	MSDI	RIP	KB
0.0	1^+	2,0,1	0.60±0.18	19.8±5.0	12.0±3.6	0.007	0.079	0.0004
		1,2,1	0.40±0.13	13.0±3.3	8.0±2.4	0.210	0.089	0.014
0.08	2^+	1,2,2	0.24±0.07	0.90±0.23	1.40±0.42	0.083	0.017	0.002
1.15	1^+	2,0,1	0.25±0.08	1.00±0.22	6.7±2.1	0.014	0.001	0.025
		1,2,1	0.25±0.08	1.00±0.25	6.7±2.1	0.001	0.011	0.061
1.32	2^+	1,2,2	0.09±0.03	2.6±0.7	1.40±0.42	0.0001	0.008	0.007
1.75	3^+	1,2,3	0.48±0.14	1.29±0.32	7.9±2.4	0.015	0.041	0.0002
		0,4,3	0.32±0.09	0.85±0.26	5.3±1.6	0.078	0.029	0.116
2.66	2^+	1,2,2	0.16±0.05	4.0±1.1	4.0±1.3	0.002	0.002	0.005
2.74	1^+	2,0,1	0.18±0.05	1.10±0.27	5.1±1.5	0.014	0.012	0.009
		1,2,1	0.29±0.09	1.60±0.27	7.6±2.3	0.154	0.018	0.030
3.00	3^+	1,2,3	0.14±0.04	1.92±0.48	1.93±0.58	0.006	0.037	0.007
		0,4,3	0.020±0.006	0.21±0.05	0.29±0.09	0.042	0.001	0.020

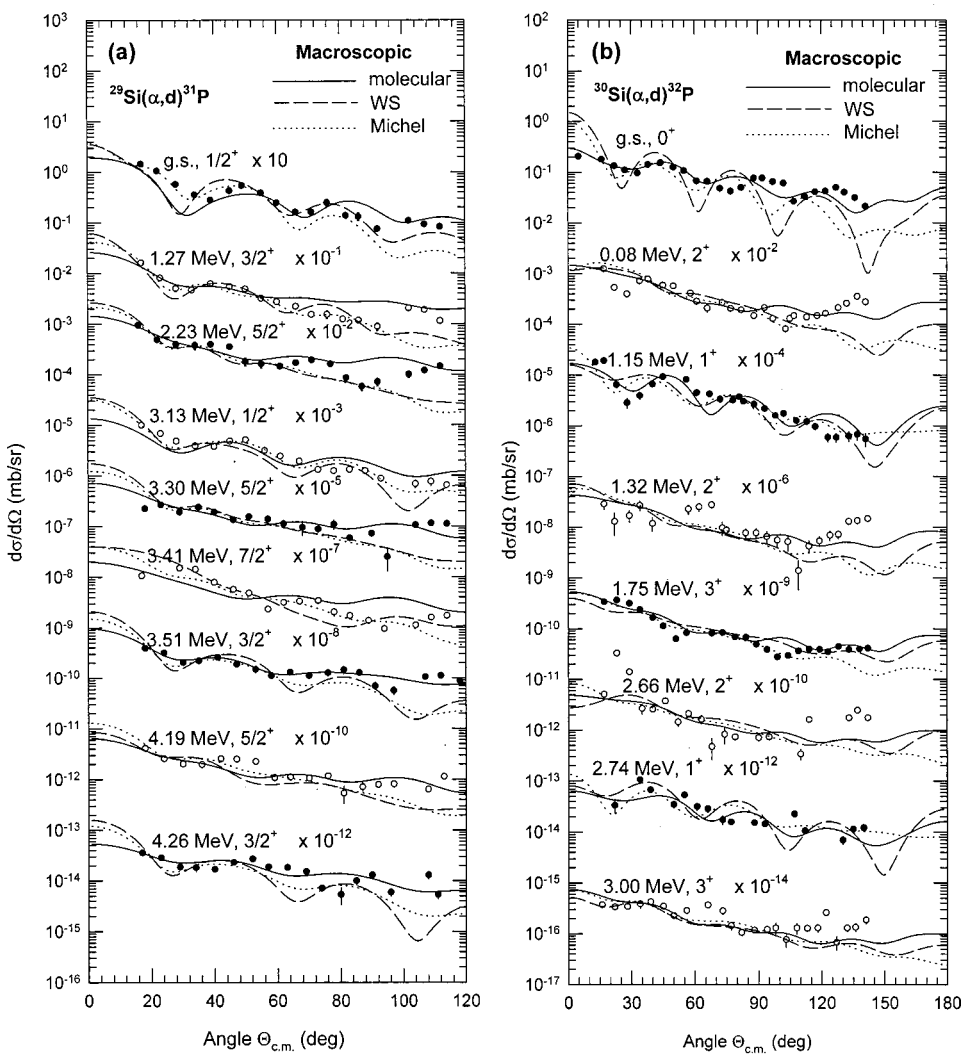

FIG. 2. Comparison of the full finite-range macroscopic DWBA calculations for the (α,d) reaction at 25 MeV leading to (a) nine even-parity states of ^{31}P and (b) eight even-parity states of ^{32}P to the differential cross-section data. The solid, broken, and dotted curves are the predictions using the molecular, standard WS, and Michel potential, respectively. Data are from Refs. [28,29].

seems to provide the best overall description of the data for the reaction on both isotopes. The deduced values of the normalization constant $\aleph$ using the spectroscopic amplitudes from all three sets of matrix elements exhibit a similar pattern and have about the same magnitude and hence, only the calculations using the MSDI spectroscopic amplitudes are presented in Table IV. The extracted $\aleph$ values for the molecular potential case vary widely and are dispersed over the range of 55 to 3800 and 600 to 4000 for the ^{29}Si$(\alpha,d)^{31}$P and ^{30}Si$(\alpha,d)^{32}$P reactions, respectively. For the ^{29}Si target where the deduced spectroscopic factors using the molecular potential compare favorably with the theoretical values calculated using shell model, the $\aleph$ values lie mostly in the range of 55 to 1100 with a mean value of $\aleph=517\pm40$. This agrees closely with the values reported in the work of de Meijer *et al.* [36]. On the other hand, the $\aleph$ values deduced using the WS and Michel potentials are larger by one to two orders of magnitude and inconsistent with the results in [36].

V. DISCUSSION

In the present work, the effects of the molecular, standard WS, and Michel types of the α-nucleus potential are examined in the analyses of the data for the two-nucleon transfer (α,d) reaction on two non-α cluster nuclei. It is as a follow-up of the same on the α-cluster nucleus ^{28}Si [26]. All three types of the α-nucleus potential for both ^{29,30}Si cases are obtained by fitting the elastic scattering data. The data of the reaction, populating nine even-parity states up to $E_x=4.26$ MeV of ^{31}P and eight even-parity states up to $E_x=3.00$ MeV of ^{32}P, have been analyzed both in terms of the FFR DWBA with the cluster form factor and the ZR DWBA with the microscopic form factors. In the latter calculations, the MSDI, RIP, and KB [28] spectroscopic amplitudes and the finite-range correction in the Gaussian form with the finite-range parameter $R=0.7$ fm are employed.

A. The ^{29}Si$(\alpha,d)^{31}$P reaction

It is evident from Fig. 2(a) that the macroscopic DWBA calculations with all three α-nucleus potentials (molecular, standard WS, and Michel) produce reasonable fits to the data of the nine transitions populating the levels of ^{31}P. The small angle data are in general better given by the Michel potential and the large angle data are better described by the molecular one. However, both the Michel and the WS potentials obtained from the best fits to the elastic scattering data fail to generate the correct order of the absolute cross sections and

TABLE III. Comparison of deduced total specstroscopic factors A from the macroscopic calculations and those S^G from the shell-model calculations using MSDI, RIP, and KB interactions [28,29].

(a) Transitions in the ^{29}Si$(\alpha,d)^{31}$P reaction

E_x	J^π	L	Total spectroscopic factors A Macroscopic calculations			Total spectroscopic factors S^G Shell-model calculations		
(MeV)			Molecular	WS	Michel	MSDI	RIP	KB
0.0	$1/2^+$	0+2	0.30±0.07	21.0±3.1	12.0±1.7	0.616	0.080	0.035
1.27	$3/2^+$	0+2	0.35±0.09	7.5±1.1	4.5±0.60	0.604	0.185	0.066
2.23	$5/2^+$	2+4	0.15±0.04	5.03±1.10	1.66±0.32	0.112	0.224	0.016
3.13	$1/2^+$	0+2	0.13±0.03	2.40±0.60	1.90±0.27	0.250	0.045	0.197
3.30	$5/2^+$	2+4	0.09±0.03	4.29±0.81	4.00±0.81	0.084	0.017	0.069
3.41	$7/2^+$	2+4	0.29±0.08	16.3±4.0	6.5±1.3	0.148	0.051	0.103
3.51	$3/2^+$	0+2	0.20±0.04	6.0±0.9	5.0±1.0	0.170	0.072	0.202
4.19	$5/2^+$	2+4	0.11±0.03	5.0±0.9	5.5±1.1	0.072	0.106	0.071
4.26	$3/2^+$	0+2	0.21±0.04	7.0±1.3	5.5±1.0	0.007	0.052	0.011

(b) Transitions in the ^{30}Si$(\alpha,d)^{32}$P reaction

E_x	J^π	L	Total spectroscopic factors A Macroscopic calculations			Total spectroscopic factors S^G Shell-model calculations		
(MeV)			Molecular	WS	Michel	MSDI	RIP	KB
0.0	1^+	0+2	1.00±0.22	32.8±6.0	20.0±4.3	0.217	0.168	0.014
0.08	2^+	2	0.24±0.07	0.90±0.23	1.40±0.42	0.083	0.017	0.002
1.15	1^+	0+2	0.50±0.11	2.00±0.33	13.3±3.0	0.015	0.012	0.086
1.32	2^+	2	0.09±0.03	2.60±0.70	1.40±0.42	0.0001	0.008	0.007
1.75	3^+	2+4	0.80±0.33	2.14±0.41	13.1±2.9	0.093	0.070	0.116
2.26	2^+	2	0.16±0.05	4.00±1.1	4.00±1.3	0.002	0.002	0.005
2.74	1^+	0+2	0.47±0.10	2.66±0.38	12.66±2.7	0.168	0.030	0.039
3.00	3^+	2+4	0.16±0.04	2.13±0.48	2.22±0.59	0.048	0.038	0.027

underestimate them by one to two orders of magnitude. This is reflected in the total spectroscopic factors deduced using these two potentials (Table III) and their comparison with the shell-model calculations. An overall good description of the angular distributions over the full angular range seems to be achieved by the molecular potential. Furthermore, the molecular potential is able to reproduce the correct order of the cross sections and yields spectroscopic factors of the same order as expected from the theoretically calculated spectroscopic amplitudes using the MSDI, RIP, and KB matrix elements.

Although, the spectroscopic factors A_L for an L transfer, deduced using the molecular potential, do not agree in most of the cases with those S_L^G calculated with the MSDI spectroscopic amplitudes (Table II), the total spectroscopic factors A using the molecular potential for all but the 4.26 MeV $(3/2^+)$ transition agree closely with those S^G predicted by the MSDI interaction (Table III). The predicted S^G and the deduced total spectroscopic factors A are in good agreement for the 2.23 $(5/2^+)$, 3.30 $(5/2^+)$, 3.51 $(3/2^+)$, and 4.19 MeV $(5/2^+)$ states and they are of the same order for the ground $(1/2^+)$, 1.27 $(3/2^+)$, 3.13 $(1/2^+)$, and 3.41 MeV $(7/2^+)$ states. The KB predictions for the 2.23 $(5/2^+)$, 3.13 $(1/2^+)$, 3.30 $(5/2^+)$, and 3.51 MeV $(3/2^+)$ states, and the RIP predictions for the 2.23 $(5/2^+)$, 4.19 $(5/2^+)$, and 4.26 MeV $(3/2^+)$ states compare closely with the total spectroscopic factors deduced using the molecular potentials.

A comparison of the microscopic DWBA calculations using the MSDI spectroscopic amplitudes for the molecular, standard WS, and Michel α-nucleus potentials with the data for all states seems to suggest that the molecular potential gives the best overall fits to the angular distributions. However, none of the potentials is able to reproduce the angular oscillations at large angles in the data for the 3.41 and 3.51 MeV states as satisfactorily as those for the other states of excitation. The Michel potential predicts larger oscillations for the ground state than required by the data. The deduced values of the normalization constant $\aleph$ in Table IV indicate clearly that the cross sections predicted by the use of the standard WS and Michel potentials are one to two orders of magnitude lower than those using the molecular potentials.

The underestimation of absolute cross sections of the (α,d) reaction by the Michel potential requires some expansion. The volume integral of its real part, $J_R/4A = 420$ MeV fm^3, is above the normally accepted range 300–400 MeV fm^3 [18,45]. In order to decrease the volume integral, one can take advantage of the "α-W_0 ambiguity" (a decrease in the value of the α parameter favors a lower value of W_0), observed by Tariq *et al.* [21]. The α parameter has been reduced to $\alpha = 4.0$, giving $J_A/4A = 342$ MeV fm^3. The

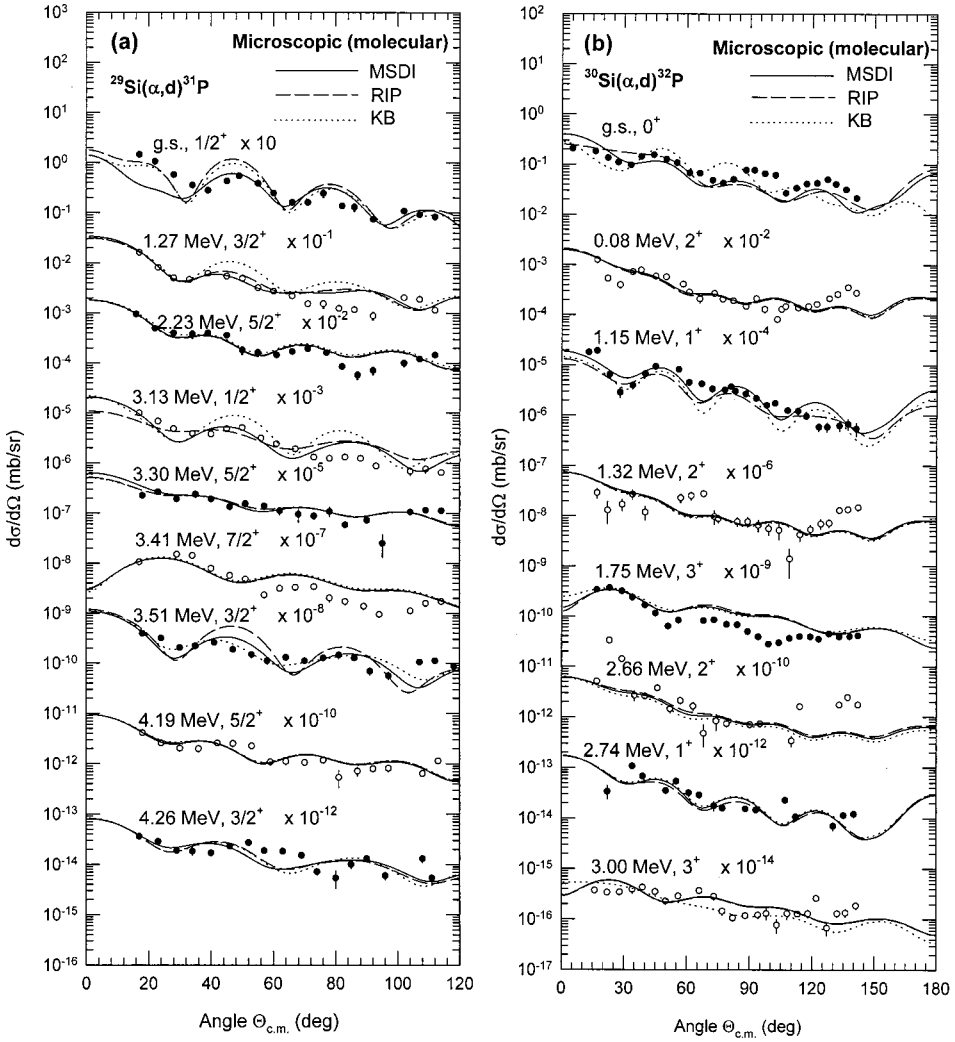

FIG. 3. Comparison of the zero-range microscopic DWBA calculations for the (α,d) reaction at 25 MeV leading to (a) nine even-parity states of ^{31}P and (b) eight even-parity states of ^{32}P to the differential cross-section data. The solid, broken, and dotted curves are the predictions using the MSDI, RIP, and KB spectroscopic amplitudes, respectively. Data are from Refs. [28,29].

corresponding best fit to the elastic data yields $W_0 = 32.0$ MeV, which enhances the absolute cross sections of the (α,d) reaction to the various final states of ^{31}P by about an order, but worsens to a great extent the fit to the oscillatory features of the angular distributions. The calculated angular distribution [broken curve in Fig. 1(a)] with $\alpha = 4.0$ and $W_0 = 32.0$ MeV produces a poorer fit to the elastic data. A further attempt to improve the elastic fit leads to $J_R/4A$ values larger than the normally accepted values.

One may feel uneasy to accept the large Coulomb radius $R_C = 9.45$ fm of the molecular potential. It is defined to be the distance between the interacting nuclei when the two barely touch each other, i.e., their densities start to overlap as noted in Ref. [27]. The sum of the two densities at $r = 9.45$ fm is about 0.005 times that of central densities. Thus, for $r > 9.45$ fm, the potential is, essentially, given by Eq. (4). It is, however, the total potential that matters. Indeed with $R_C = 3.99$ fm, the Michel value, one can generate the same potential for the real part of the molecular potential with equivalent parameters: $V_0 = 27.7$ MeV, $R_R = 5.45$ fm, $a_R = 0.363$ fm, $V_1 = 37.9$ MeV, and $R_1 = 2.78$ fm. These new values, which are acceptable, coupled with the unadjusted parameters of the imaginary parts produce identical fits to the data of the (α,d) reaction as well as the elastic scattering. However, at $R_C = 3.99$ fm, used in the Michel potential, the overlap of the densities of the two colliding nuclei is substantial and hence, it does not reflect the usual definition of the Coulomb radius.

B. The ^{30}Si$(\alpha,d)^{32}$P reaction

Figure 2(b) shows that the macroscopic DWBA calculations with all three α-nucleus potentials (molecular, standard WS, and Michel) produce reasonable fits to the data of all transitions except the one to the 2.66 MeV (2^+) state of ^{32}P. The fits to the angular distribution data leading to the ground (1^+), 1.15 (1^+), and 1.75 MeV (3^+) states in ^{32}P with the molecular potential are particularly good, which is not the case for the WS and Michel potentials. On the other hand, the Michel potential does better in reproducing the data for the 1.32 (2^+) and 2.74 MeV (1^+) states compared to the molecular and WS potentials. The total spectroscopic factors A, deduced using the standard WS and Michel potentials, are larger than those extracted using the molecular potential by at least an order of magnitude. In general, the deduced spectroscopic factors for the case of the molecular potential are in agreement with those calculated by the shell model, in particular, on whether a transition is strong or weak. This means

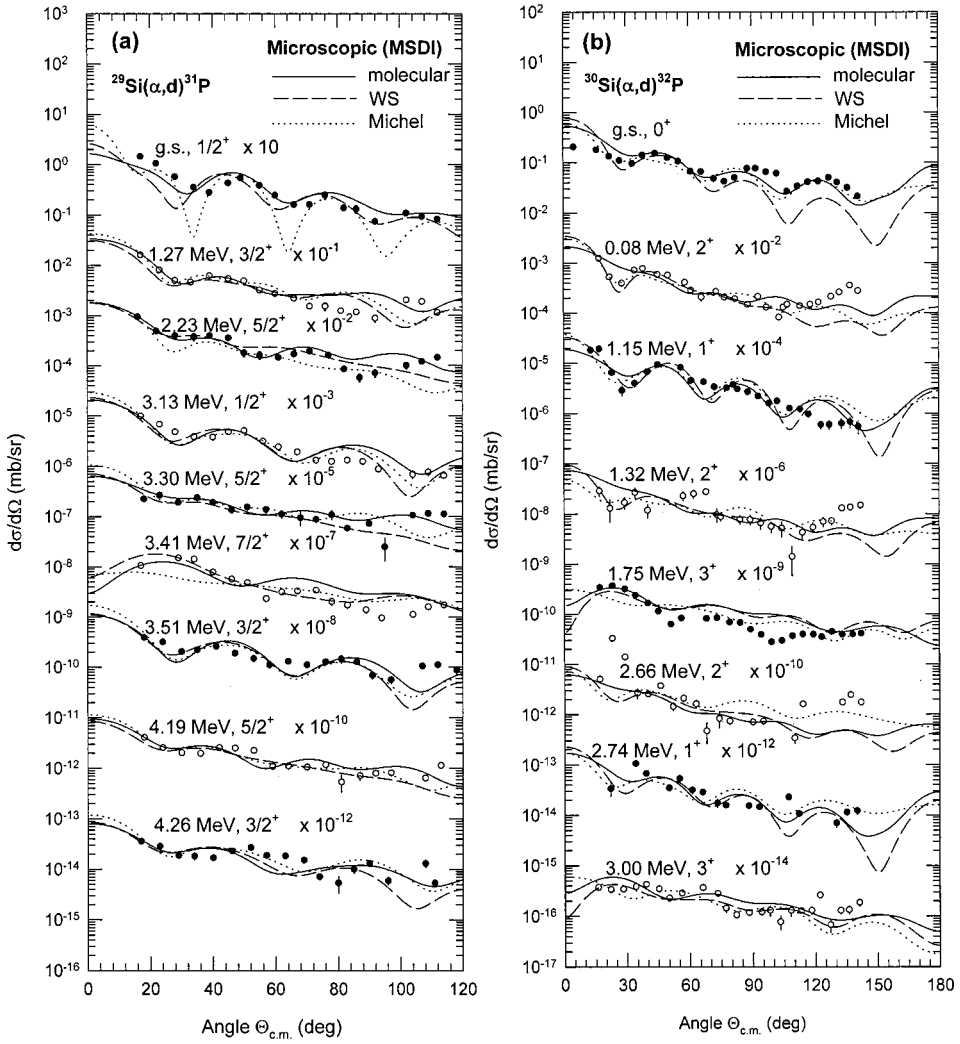

FIG. 4. Same as in Fig. 2 for the zero-range microscopic DWBA calculations.

that the calculated cross sections using both the WS and Michel potentials are smaller in magnitude by at least an order. The deduced total spectroscopic factors A for the case of the molecular potential are sometimes slightly higher than those, S^G, predicted by the shell-model calculations. If one compares the deduced spectroscopic factors using the molecular potential with those calculated with the MSDI spectroscopic amplitudes, one can note that for a good number of cases, namely, the transitions to the ground (1^+), 0.08 (2^+), 2.74 (1^+), and 3.00 MeV (3^+) states, the discrepancy is approximately a factor of 0.3. For the other transitions using the MSDI spectroscopic amplitudes and for all the transitions

TABLE IV. Comparison of values of the normalization constant for the (α,d) reaction deduced from the microscopic calculations using the MSDI spectroscopic amplitudes [28,29].

^{29}Si$(\alpha,d)^{31}$P					^{30}Si$(\alpha,d)^{32}$P				
E_x (MeV)	J^π	Normalization constant ℵ			E_x (MeV)	J^π	Normalization constant ℵ		
		Molecular	WS	Michel			Molecular	WS	Michel
0.0	$1/2^+$	55	900	550	0.0	1^+	4000	48000	60000
1.27	$3/2^+$	500	6000	3200	0.08	2^+	600	6000	8000
2.23	$5/2^+$	400	6500	1900	1.15	1^+	4000	40000	60000
3.13	$1/2^+$	80	1200	550	1.32	2^+	2300	20000	30000
3.30	$5/2^+$	180	4000	2200	1.75	3^+	3800	8000	60000
3.41	$7/2^+$	800	14000	800	2.66	2^+	700	7000	15000
3.51	$3/2^+$	1100	15000	80000	2.74	1^+	1700	15000	25000
4.19	$5/2^+$	3800	50000	22000	3.00	3^+	1500	7000	3000
4.26	$3/2^+$	590	11000	59000					

with the RIP and KB amplitudes, the disagreement between the calculated S^G and the deduced spectroscopic factors A is somewhat larger.

The microscopic DWBA calculations using the MSDI spectroscopic amplitudes listed in Fig. 4(b) show that the molecular, standard WS, and Michel potentials generate reasonable fits to the data for all of the transitions except that to the 1.75 MeV state, where the quality of fit is poor, and that to the 2.66 MeV state, where the predictions are far from the data as observed in the macroscopic analysis. Although the Michel potential does fit the small angle data for the 0.08 and 1.15 MeV states better, the molecular potential seems to provide the best overall fit. The deduced values of the normalization constant $\aleph$ in Table IV indicate once again that the standard WS and Michel potentials underestimate the cross sections by at least an order of magnitude, while the molecular potential reproduces the correct order. The failure of both the microscopic and macroscopic calculations to account for the angular distribution for the 2.66 MeV state may lie in the substantial contribution of two-step processes via the excitation of the inelastic states of ^{30}Si.

The parameters of the Michel potential give $J_R/4A = 517$ MeV fm^3. In order to examine the effect of reducing the volume integral to an acceptable level, the value of the α-parameter has been reduced to $\alpha = 4.0$. The corresponding best-fit to the elastic data results in $W_0 = 24.0$ MeV, which yields $J_R/4A = 379$ MeV fm^3. However, the calculated cross sections [broken curves in Fig. 1(b)] result in an unsatisfactory fit to the elastic data beyond 100° scattering angles. With the new set of parameters, the calculated cross sections for the (α,d) reaction increase at best by an order of magnitude, but the fit to the angular oscillations become much worse.

An equivalent set of parameters for the real part of the molecular potential for $R_C = 4.04$ fm, the Michel value, has been obtained as $V_0 = 28.4$ MeV, $R_R = 5.52$ fm, $a_R = 0.362$ fm, $V_1 = 37.5$ MeV, and $R_1 = 2.78$ fm. This new set of values with the unadjusted parameters of the imaginary part again produces identical fits to the data of the (α,d) reaction as well as the elastic scattering.

VI. CONCLUSION

Both the macroscopic and microscopic DWBA analyses carried out here seem to suggest the preference for the molecular type of the α-nucleus potential. The angular distributions in almost all cases can be described successfully without the inclusion of the compound nucleus contribution that Jankowski *et al.* [37] had to do in the case of the ^{28}Si$(\alpha,d)^{30}$P reaction, and without having to adjust any of the parameters of the α-nucleus potential, obtained from fitting the elastic data, that Davis and Nelson [28] apparently failed to achieve.

The macroscopic spectroscopic factors for the cluster transfer in the (α,d) reactions as introduced by Skwirczynska *et al.* [46] and de Meijer *et al.* [36] are found to be strongly dependent on the nature of the α-nucleus potential and are sensitive to the shell-model interaction from which the spectroscopic amplitudes are extracted. Hence, the cluster spectroscopic factor is a sensitive probe not only to examine the α-nucleus potential but also to test the shell-model interaction. The present work suggests that the MSDI interaction is the best of the three shell-model interactions considered herein for silicon and phosphorus.

In consonance with the finding of our previous works on the ^{28}Si$(\alpha,d)^{30}$P reaction [26] and the ^{28}Si$(\alpha,p)^{31}$P reaction [27], one may summarize that while the molecular potential with a repulsive core, the Michel potential with squared WS geometry, and the standard optical potential with the WS shape produce more or less similar quality fits to the elastic scattering data (Fig. 1); they lead to a significantly different scenario in the description of the two-nucleon (α,d) and the three-nucleon (α,p) transfer reactions. The Michel and standard WS potentials are found to underestimate the cross sections of these reactions by one to four orders of magnitude. The predictions for the (α,d) reactions with the Michel potential are, however, very much sensitive to the volume integral $J_R/4A$ of the real part of the α-nucleus potential. In the present study the volume integrals 420 and 517 MeV fm^3 for the ^{29,30}Si nuclei, respectively, are larger than the accepted range 300–400 MeV fm^3 [18,45]. Reduction of the integral through the use of the so-called α-W_0 ambiguity [21] leads to an enhancement of absolute cross sections of the (α,d) reaction by about an order of magnitude at the cost of providing a much worse fit to the oscillatory features of the angular distributions of the reaction as well as the α elastic scattering. The apparent unsatisfactory performance of the Michel potential in the description of the (α,d) reaction may lie in its α-W_0 ambiguity. It remains to be seen whether a Michel potential within the acceptable range of the volume integral can describe the α elastic and the (α,d) reaction data simultaneously. The molecular α-nucleus potential reproduces simultaneously the right magnitude of experimental cross sections and the correct structures of angular oscillations of the data quite satisfactorily. Since both (α,d) and (α,p) reactions have a large angular momentum mismatch due to their large negative reaction Q values, a substantial contribution to the cross sections from the nuclear interior is expected, making these reactions sensitive to the details of the α-nucleus potential. Thus, although the molecular, standard WS, and Michel potentials may produce similar effective potentials responsible for the elastic scattering, which primarily probes the nuclear surface, their divergent forms in the nuclear interior have an important impact on the nonelastic processes. This supports Satchler's contention [47] that the real test of a potential lies in its ability to reproduce elastic and nonelastic data simultaneously. A simultaneous analysis of all relevant reactions may lead to a global α-nucleus potential [48]. However, for a meaningful analysis, data on the complete angular distribution are also needed as observed by Budzanowski *et al.* [49]. The success of the molecular potential conforms to Baye's [50] assertion that amongst the phase equivalent potentials, a shallow potential with a singularity, to which the molecular potential closely bears resemblance, eliminates the states forbidden by

the Pauli principle and is, therefore, expected to produce a better description of the reaction data.

The present work in conjunction with the previous studies of the α-elastic scattering on ^{24}Mg and ^{28,30}Si by Tariq *et al.* [21], the (α,t) reaction on ^{27}Al [22], the (α,d) [26] and (α,p) [27] reactions on ^{28}Si by Das *et al.*, and the α inelastic scattering on ^{24}Mg and ^{28}Si by Basak *et al.* [25] confirms that of the three types of α-nucleus interactions considered in all cases, the molecular potential describes the data so far best. Some of the poor fits may be attributed to the fact that the spectra of ^{31}P and ^{30}P, a neighboring odd-odd nucleus, are well reproduced by the Coriolis coupling model, implying deformation [51,52] in these nuclei. The exisitng shell-model codes are not in a position to deal with this issue.

ACKNOWLEDGMENTS

This work was partly supported by Grant No. INT-9808892 of the U.S. National Science Foundation and a grant from the Ministry of Science and Technology, Government of Bangladesh, which are gratefully acknowledged. The authors are thankful to Professor J.M. Nelson of the University of Birmingham and Dr. N. Davis of the University of Staffordshire, England for sending the tabular form of α elastic cross sections and the spectroscopic amplitudes and to Professor P.D. Kunz of the University of Colorado for making the codes DWUCK4 and DWUCK5 available to them. One of the authors, S.K.D., is also thankful to Shahjalal University of Science and Technology, Bangladesh for the study leave grant.

[1] J.C. Correlli, E. Bleuler, and D.J. Tendam, Phys. Rev. **116**, 1184 (1959).
[2] C.R. Gruhn and N.S. Wall, Nucl. Phys. **81**, 161 (1966).
[3] G. Gaul, H. Lüdeke, R. Santo, H. Schmeing, and R. Stock, Nucl. Phys. **A137**, 177 (1969).
[4] A. Bobrowska, A. Budzanowski, K. Grotowski, L. Jarczyk, S. Micek, H. Niewodniczanski, A. Strzalkowski, and Z. Wróbel, Nucl. Phys. **A126**, 361 (1969).
[5] H. Eickhoff, D. Frekers, H. Lönner, K. Poppensieker, R. Santo, G. Gaul, C. Mayer-Böricke, and P. Turek, Nucl. Phys. **A252**, 333 (1975).
[6] H. Abele, H.J. Hauser, A. Körber, W. Leitner, R. Neu, H. Plappert, T. Rohwer, G. Staudt, M. Straßer, S. Welte, M. Walz, P.D. Eversheim, and F. Hinterberger, Z. Phys. A **326**, 373 (1987).
[7] W. Trombik, K.A. Eberhard, and J.S. Eck, Phys. Rev. C **11**, 685 (1975).
[8] A.M. Kobos, B.A. Brown, R. Lindsay and G.R. Satchler, Nucl. Phys. **A425**, 205 (1984).
[9] R. Stock, G. Gaul, R. Santo, M. Bernas, B. Harvey, D. Hendrie, J. Mahoney, J. Sherman, J. Steyaert, and M. Zisman, Phys. Rev. C **6**, 1226 (1972).
[10] H. Oeschler, H. Schroter, H. Ficjs, L. Baum, G. Gaul, H. Ludechi, R. Santo, and R. Stock, Phys. Rev. Lett. **28**, 694 (1972).
[11] Å. Bredbacka, M. Brenner, K.-M. Källman, P. Manngård, Z. Máté, S. Szilágyi, and L. Zolnai, Nucl. Phys. **A574**, 397 (1994).
[12] L. Jarczyk, B. Maciuk, M. Siemaszko, and W. Zipper, Acta Phys. Pol. B **7**, 531 (1976).
[13] H.-J. Apell, W. Gemeinhardt, R. Stock, R.R. Betts, O. Hansen, A. Sperduto, H. Fuchs, and R. Santo, Nucl. Phys. **A246**, 477 (1975).
[14] A.W. Obst and K.W. Kemper, Phys. Rev. C **6**, 1705 (1972).
[15] A.E. Antropov, S.I. Vasilev, P. Zurabin, and B.N. Orlov, Izv. Akad. Nauk SSSR, Ser. Fiz. **38**, 2175 (1974); **37**, 1873 (1973).
[16] M. Brenner, in *Clustering Phenomena in Atoms and Nuclei*, edited by M. Brenner, T. Lönnroth, and F. B. Malik (Springer-Verlag, Berlin, 1992), p. 327.
[17] Th. Delbar, Gh. Grégoire, G. Paic, R. Ceuleneer, F. Michel, R. Vanderpoorten, R. Budzanowski, H. Dabrowski, L. Friendl, K. Grotowski, S. Micek, R. Planeta, A. Strzalkowski, and A. Eberhard, Phys. Rev. C **18**, 1237 (1978).
[18] F. Michel, J. Albinski, P. Belery, Th. Delber, Gh. Grégoire, B. Tasiaux, and G. Reidemeister, Phys. Rev. C **28**, 1904 (1983).
[19] F. Michel, G. Reidemeister, and S. Ohkubo, Phys. Rev. Lett. **57**, 1215 (1986).
[20] F. Michel, G. Reidemeister, and Y. Kondo, Phys. Rev. C **51**, 3290 (1995).
[21] A.S.B. Tariq, A.F.M.M. Rahman, S.K. Das, A.S. Mondal, M.A. Uddin, A.K. Basak, H.M. Sen Gupta, and F.B. Malik, Phys. Rev. C **59**, 2558 (1999).
[22] S.K. Das, A.S.B. Tariq, A.F.M.M. Rahman, P.K. Roy, M.N. Huda, A.S. Mondal, A.K. Basak, H.M. Sen Gupta, and F.B. Malik, Phys. Rev. C **60**, 044617 (1999).
[23] I. Reichstein and F.B. Malik, Phys. Lett. **37B**, 344 (1971).
[24] P. Manngård, M. Brenner, M.M. Alam, I. Reichstein, and F.B. Malik, Nucl. Phys. **A504**, 130 (1989).
[25] A.K. Basak, A.S.B. Tariq, S.K. Das, A.F.M.M. Rahman, A.S. Mondal, H.M. Sen Gupta, and F.B. Malik (unpublished).
[26] S.K. Das, A.S.B. Tariq, M.A. Uddin, A.S. Mondal, A.K. Basak, K.M. Rashid, H.M. Sen Gupta, and F.B. Malik, Phys. Rev. C **62**, 054605 (2000).
[27] S.K. Das, A.K. Basak, K. Banu, A.S. Mondal, A.S.B. Tariq, A.F.M.M. Rahman, H.M. Sen Gupta, and F.B. Malik, Phys. Rev. C **62**, 054606 (2000).
[28] N.J. Davis and J.M. Nelson, Nucl. Phys. **A458**, 475 (1986).
[29] J.M. Nelson and N.J. Davis (private communication).
[30] F. James and M. Roos, Comput. Phys. Commun. **10**, 343 (1975).
[31] O. Bersillon, Code SCAT2, NEA 0829.
[32] I.S. Towner and J.C. Hardy, Adv. Phys. **18**, 401 (1969).
[33] N.K. Glendenning, Phys. Rev. **137**, B102 (1965).
[34] M. K. Pal, *Theory of Nuclear Structure* (Affiliated East-West Press, New Delhi, 1982).
[35] P. D. Kunz, codes DWUCK4 and DWUCK5.
[36] R.J. de Meijer, L.W. Put, J.J. Akerman, J.C. Vermeulen, and C.R. Binham, Nucl. Phys. **A386**, 200 (1982).
[37] K. Jankowksi, A. Grzeszczuk, M. Siemanszko, A. Surowiec, W. Zipper, A. Budzanowski, and E. Kozik, Nucl. Phys. **A426**, 1 (1984).
[38] N. K. Glendenning, in *Nuclear Spectroscopy and Reactions, Part D*, edited by J. Cerny (Academic Press, New York, 1975), p. 319.

[39] W. Fitz, J. Heger, R. Santo, and S. Wenneis, Nucl. Phys. **A143**, 113 (1970).
[40] L.A. Charlton, Phys. Rev. C **8**, 146 (1978).
[41] T.T.S. Kuo and G.E. Brown, Nucl. Phys. **85**, 40 (1966); T.T.S. Kuo, Nucl. Phys. **A103**, 71 (1967).
[42] T. Hamada and I.D. Johnston, Nucl. Phys. **134**, 382 (1962).
[43] E.C. Halbert, J.B. McGrory, B.H. Wildenthal, and S.P. Pandya, Adv. Nucl. Phys. **4**, 315 (1971).
[44] B.H. Wildenthal and J.B. McGrory, Phys. Rev. C **7**, 714 (1973).
[45] F. Michel and G. Reidemeister, Phys. Rev. C **62**, 049801 (2000).
[46] I. Skwirczynska, E. Kozik, A. Budzanowski, J. Ploskonka, and A. Strzalkowski, Nucl. Phys. **A371**, 288 (1981).
[47] G. R. Satchler, in *Proceedings of the International Conference on Reactions between Complex Nuclei*, edited by R. L. Robinson *et al.* (North-Holland, Amsterdam,1974), p. 171.
[48] P. E. Hodgson, Oxford Report No. OUNP-94-09 (1994).
[49] A. Budzanowski, L. Jarczyk, L. Kamys, and A. Kapuscik, Nucl. Phys. **A265**, 461 (1976).
[50] D. Baye, Phys. Rev. Lett. **58**, 2738 (1987).
[51] F. B. Malik and W. Scholz, in *Nuclear Structure*, edited by A. Hussain *et al.* (North-Holland, Amsterdam, 1974), p. 34.
[52] P. Wasielewski and F.B. Malik, Nucl. Phys. **A160**, 113 (1971).